**IJCTA**, 9(31), 2016, pp. 329-345 ISSN: 0974-5572

# Modeling and Dynamic Analysis of Six Phase Self Excited Induction Generator for Static Load Condition

**Mabujohn L.* and A. Senthilkumar****

**ABSTRACT**

This paper presents a simple d–q model of isolated six phase self excited induction generator (SPSEIG) driven by a fixed pitch wind turbine. The mathematical modeling and dynamic performance of common mutual leakage inductance between the two three-phase winding sets has been studied. The proposed simulation is based on a wind-turbine model, SPSEIG model and detailed transient behavior of an SPSEIG for sudden switching of various static load conditions on both the winding sets. The analysis of detailed computer model has been developed in an arbitrary reference frame for various performances including loading and unloading characteristics, power capability and reliability of power generating system. The simulation results show a SPSEIG performance and also the transient response under different load condition with and without series compensation. Thus, the modeling of six phases self excited induction generator and performances are verified using MATLAB/SIMULINK software.

***Keywords***: D-Q Model, Dynamic analysis, Series Compensation, Six Phases Self Excited Induction Generator (SPSEIG), Various Static Load Condition, Wind Turbine.

## 1. INTRODUCTION

Recently, the Multi-phase AC machines are widely considered as potentially viable solutions for numerous variable-speed drive applications. Due to increase the emphasis on renewable electric energy generation, while interfacing with the grid takes place by means of power electronic converters are used for stand-alone applications. The dynamic analysis of SEIG supports the operation for different network operating conditions. The induction generator is used in wind energy conversion systems and corresponding rotational speed depends upon the wind speed. The good performance of machine based on careful selection of shunt and series capacitance for excitation process. The design SEIG based single phase load for standalone systems using MATLAB software [1, 2]. In this literature presented a d-q modeling of saturated multi-phase (six-phase) self-excited induction generator for renewable energy generation. In order to investigation of various condition such as include the voltage build up, collapse of voltage and various performance admitting loading and unloading characteristic of power capability and reliability for power generating system. The steady state performances of SEIG have been compared with experimental results for different configuration [3].

The dynamic model of multi-phase induction machines consisting of two identical three-phase stator windings sets sharing the same magnetic circuit. The analytic model has developed in general arbitrary reference frame. In this model is most suitable for analysis of generator behavior with an arbitrary angle of displacement between the two three-phase winding sets. The simulation a result has been obtained from effectively utilized for balanced as well as unbalanced load conditions. The proper selection of series

---

* Research Scholar, Department of Electrical and Electronics Engineering, Anna University, Chennai, India, *Email: mabujohnphd123@gmail.com*

** Professor, Department of Electrical and Electronics Engineering, Velammal Engineering College, Chennai, India,*Email: vastham@gmail.com*

capacitors is used for the voltage regulation profile improvement of SEIG. So it becomes provide the additional VAR requirement with increase of load current. This combination of series and shunt capacitors are necessary to achieve the desired level of voltage regulation for keeping the machine voltage and current within specified limits [4, 5]. The mathematical representation of n phase induction machines are normally applied for high power applications such as ship propulsion, electric aircraft and electric/hybrid electric vehicles. The developed model based power generating system of magnetizing inductance saturation and excitation capacitors for task of excitation [6, 7].

The number of balanced and unbalanced capacitors, passive and active load analysis of self-excited induction generator connected to a load either directly or by an intermediate of a power converter. The main reason of the decrease in generator rotational speed depends upon the change in load torque. Also, this frequencies result slightly decrease while after the load application is detected. The transfer function method is used to analyze the propagation of harmonic currents generated by nonlinear load to the stator windings of SEIG [8, 9]. The IEEE Standard for Rotating Electric Machinery for Rail and Road Vehicles application referred in IEEE Std 11-2000. The voltage regulation of SEIG terminal voltage can be maintained constant and free from harmonics under linear/non linear and balanced/unbalanced loads using STATCOM. It is also used for the harmonic elimination and provides the required reactive power for load balancing. The excitation capacitances cause the generated voltage to delay a moment to reach its steady-state value [10, 11].

The wind turbine based self excited induction generator is used to track and extract maximum power to the grid. The reactive power compensation can be achieved by using the constant voltage and variable frequency based converter. The selection of capacitor is based on the frequency and magnetic reactance and the independent variables depending upon the operational condition of the machine [12, 13]. The performance of multi-pulse electronic load controller (ELC) based isolated asynchronous generator (IAG) for improvement of power quality. The simulation results can be carried out the THD (Total Harmonic Distortion) is evaluated based on FFT (Fast Fourier Transformation). The comparison between different terminal capacitor connections based renewable energy applications in remote locations, while feeding single-phase loads (IEEE Std 114-2001). This load is depending upon maximum load expected to be served, variations in voltage and frequency that can be tolerated and reactive power requirements [14, 15].

In this paper, presents the dynamic performance of an isolated 6 phase self excited induction generator (SPSEIG) driven by a fixed pitch wind turbine. The SPSEIG performance has been analyzed and verified at under various static load conditions. The effect of series compensation have been analyzed for both three-phase winding sets abc and xyz. The voltage/current regulation, power handling capability and efficiency of power generating system have been verified.

## 2. WIND TURBINE MODEL

In general, fixed pitch wind turbine has been modeled to drive induction generator. It becomes used to isolate the effects of electrical control rather than mechanical control because pitch control is achieved through hydraulic manipulation. The number of blades are taken as 3 blade radius equal to considered as 13m and also similarly the gear ratio is taken as 30 with fixed pitch as . Hence, the power coefficient characteristic of wind turbine explain the non-linear curve that reflects the aerodynamic behavior. In order to make the wind turbine model compatible with real value components, several modifications can be applicable in the Simulink wind turbine model. First one consider the wind turbine model was changed from a per unit system to the actual value system. Second one contains the variable pitch model was changed to fixed pitch turbine. According to this purpose, the value of the pitch angle is set to zero. The characteristic forms the basis for the custom turbine model (IEEE standard 519). The non-linear dimensionless Cp characteristic is given as,

$$C_p(\lambda,\beta)=c_1\left(c_2/\lambda_i-c_3\beta-c_4\right)e^{-c_5/\lambda_i}+c_6\lambda_i \tag{1}$$

$$1/\lambda_i=1/\lambda+0.08\beta-0.035/\beta^3+1 \tag{2}$$

The values are $c_1=0.5176, c_2=116, c_3=0.4, c_4=5, c_5=21, c_6=0.0068$. The new power coefficient is derived from above equation is given by,

$$C_p(\lambda)=0.5176\left(116/\lambda-\left(116*0.035\right)-5\right)e^{-21/\lambda-21*0.035}+0.0068\lambda \tag{3}$$

The different values of the pitch angle β to represent the performance of $C_p(\lambda)$ characteristics are shown above in figure 1.

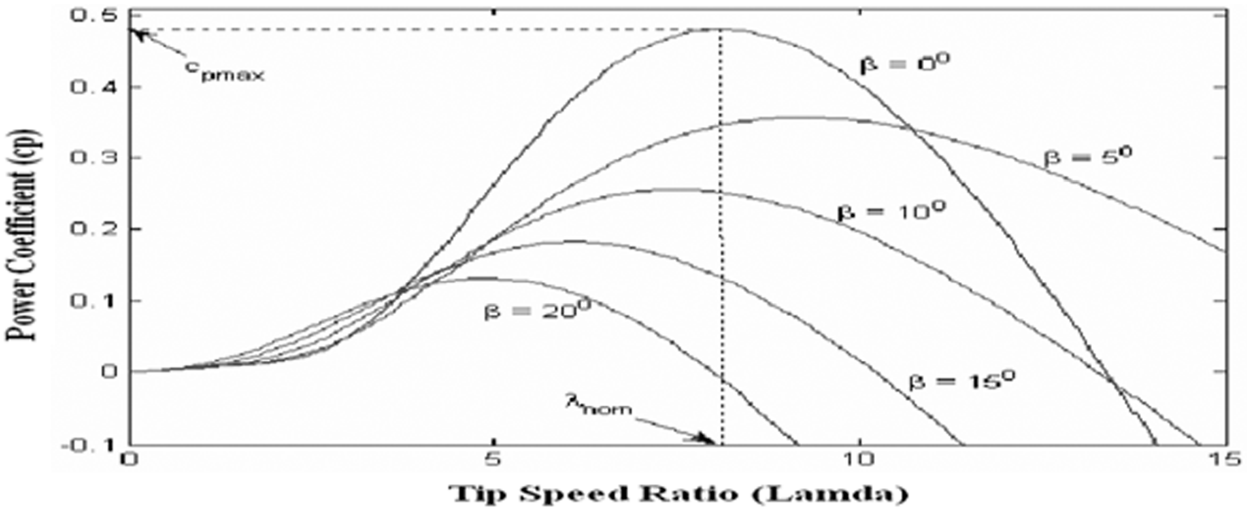

**Figure 1: $C_p$ Characteristics of wind turbine**

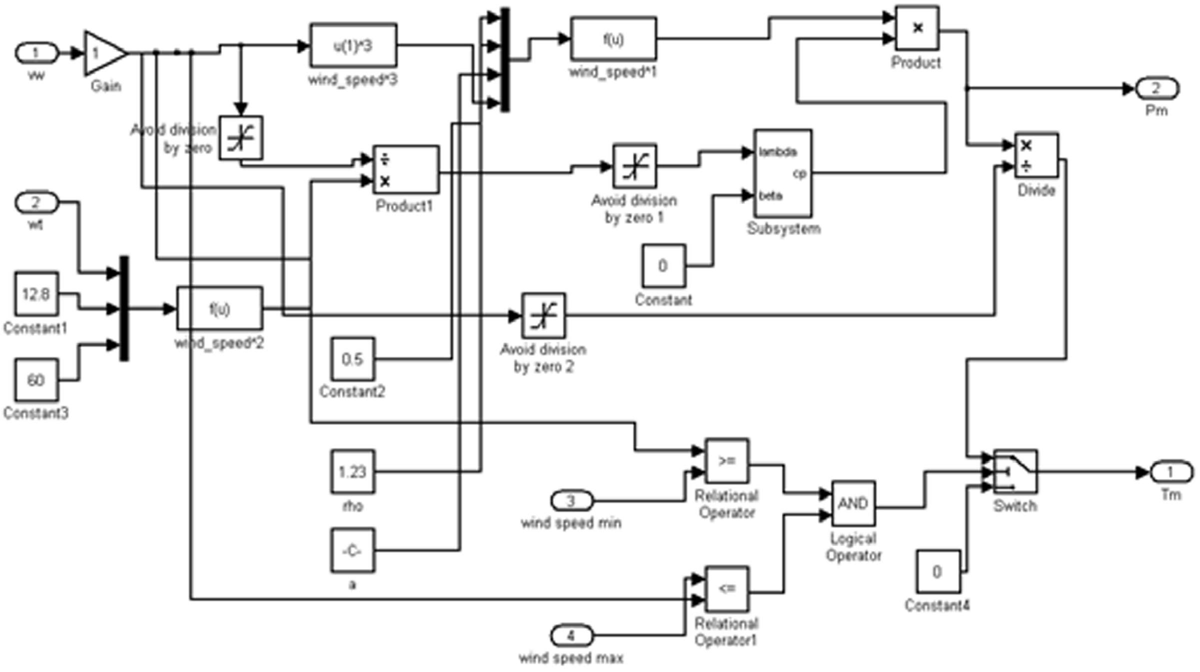

**Figure 2: Simulink Model of custom wind turbine**

The torque and power characteristic of wind turbine as represent by following equations such as, $W_w$ is Turbine rotor speed or angular velocity and V is Wind speed of turbine.

$$T_m = P_m / W_w \tag{4}$$

$$P_m = C_p(\lambda, \beta) 0.5 \rho A V^3 \tag{5}$$

The $C_p$ can be obtained by developing the custom wind turbine model in Matlab Simulink. The Simulink Model of wind turbine is shown above in figure 2.

## 3. SELF EXCITED INDUCTION GENERATOR (SEIG)

Induction machine (IM) is quite popular with isolated several advantages to hydro and wind power plants compare to other generators available in the market. It is a singly-excited ac machine construction, self-start quality, low maintenance and low cost draw greater attention from the last decades of WESs developers. It has also been more rugged, requiring no brushes or commutator. Based on the slip value, the induction machine can be worked in motor as well as generator mode of operation. In motoring mode of operation (0 < slip < 1), the rotor rotates in the direction of rotating field produced by the stator currents. The slip varies from 1 at stand still to 0 at synchronous speed. But in generating mode of operation (-1 < slip < 0), the stator terminals are connected to a constant frequency voltage source and rotor is driven at above synchronous speed by a prime mover (IEEE Std 112-2004). The self excited may be occurring under favorable conditions, while the suitable capacitance is connected across the stator winding of the induction machine. It has been order to supply the necessary reactive power to achieve generating electrical energy in remote areas. This operating mode of operation is called as Self Excited Induction Generator (SEIG).

The process of self excited induction generator with graphical representation is shown above in figure 3. It has found increasing applications in distributed generating system utilizing renewable energy. This machine is ideal choice for electricity generation in variable speed wind energy conversion system. Because it's reactive power from the grid is not available. In mode operation, the induction generator needs a reasonable amount of reactive power which can be fed externally to establish the magnetic field necessary to convert the mechanical power from its shaft into electrical power. An appropriate choice of excitation capacitance is required in order to achieve the initiate voltage build up and maintain a given terminal voltage when the SEIG is loaded.

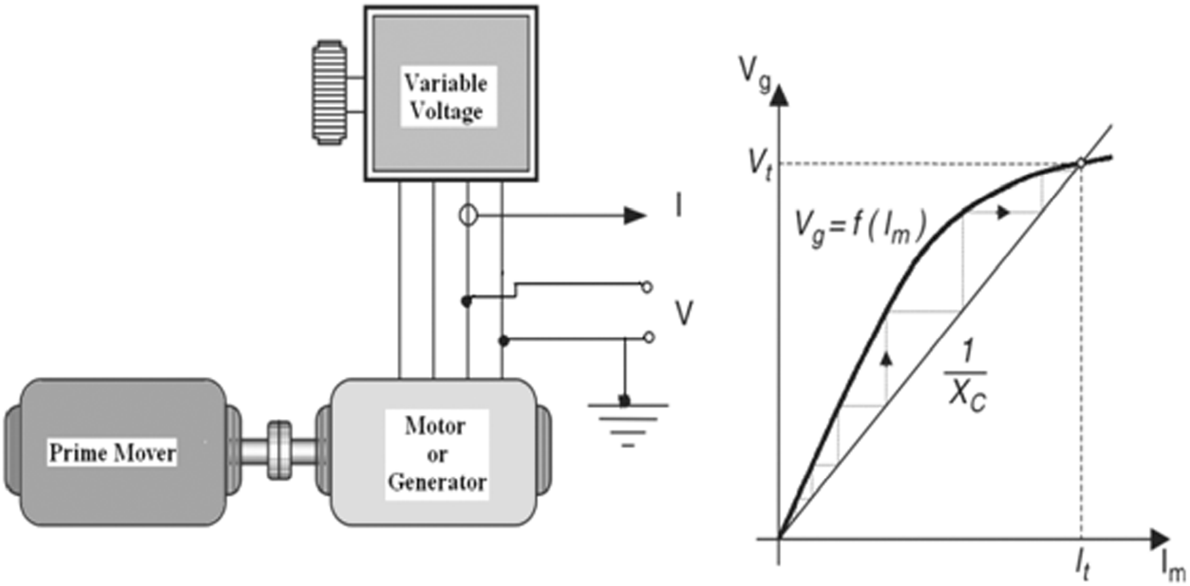

Figure 3: Self excited process of induction generator.

## 4. SP-SEIG MATHEMATICAL MODEL

In order to increase of efficiency as the number of phases increase is attributed in self excited induction generator. So that power delivery becomes more continuous such as the number of phases increases. The transient model of induction generator is exactly similar to an induction motor. The only difference between these two contains in placing a minus sign before the current phase symbolizing the generator mode instead of a motor. Also, the model of the six-phase self excited induction generator (SPSEIG) can be easily pointed-out based on the six-phase motor. Here, the stator winding is separated into two identical three-phase winding sets. The usage of Park transformation can be applied to each three-phase set separately for adopting the usual simplification model.

The schematic representation of two pole six phase machine is shown above in figure 4. The stator has been distributed six phase windings such as a, b, c and x, y, and z. It has connected in set of two stars with isolated neutral for prevent the flow of triplen harmonics and physical fault between the two stator winding sets. The magnetic axes of the two winding three-phase sets are displaced by an angle of 30 electrical degrees. It should be assumed that the windings of each set sinusoidal distributed and have corresponding axes displaced by 120 degrees. The three-phase rotor windings $a_r$, $b_r$, $c_r$ are also sinusoidal distributed and also the corresponding axes are displaced by 120 degree. In developing the above equations describe the behavior of a multi phase machine assumed. Here, it is not control the physical fault propagation from one three phase set to the other three phase set.

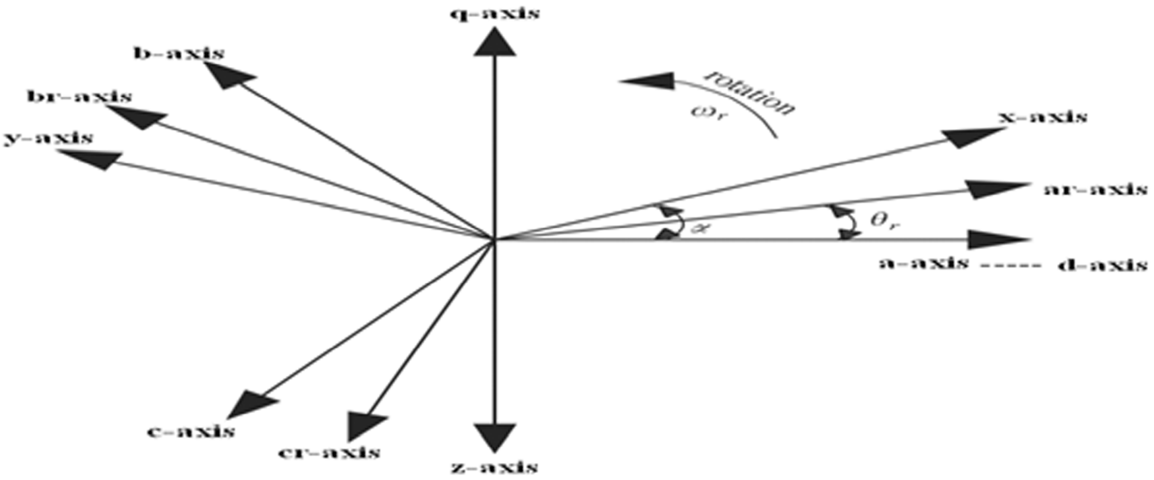

**Figure 4: Schematic Diagram of two pole six phase induction machine**

The voltage equations in the arbitrary reference frame of multiphase induction machine are given by,

$$V_{q1} = -r_1 i_{q1} + \omega_k \lambda_{d1} + p\lambda_{q1} \tag{6}$$

$$V_{d1} = -r_1 i_{d1} - \omega_k \lambda_{q1} + p\lambda_{d1} \tag{7}$$

$$V_{q2} = -r_2 i_{q2} + \omega_k \lambda_{d2} + p\lambda_{q2} \tag{8}$$

$$V_{d2} = -r_2 i_{d2} - \omega_k \lambda_{q2} + p\lambda_{d2} \tag{9}$$

$$0 = r_r i_{qr} + [\omega_k - \omega_r]\lambda_{dr} + p\lambda_{qr} \tag{10}$$

$$0 = r_r i_{dr} - [\omega_k - \omega_r]\lambda_{qr} + p\lambda_{dr} \tag{11}$$

Where, $\omega_k$ is speed of the reference frame, p represent the differentiation of time, $\omega_r$ is rotor speed and all other symbols declare that usual meaning. Here, rotor quantities are referred to stator. The expressions of stator and rotor flux linkages are given below,

$$\lambda_{q1} = -L_{11} i_{q1} - L_{lm}\left[i_{q1} + i_{q2}\right] + L_m\left[-i_{q1} - i_{q2} + i_{qr}\right] \tag{12}$$

$$\lambda_{d1} = -L_{11} i_{d1} - L_{lm}\left[i_{d1} + i_{d2}\right] + L_m\left[-i_{d1} - i_{d2} + i_{dr}\right] \tag{13}$$

$$\lambda_{q2} = -L_{12} i_{q2} - L_{lm}\left[i_{q1} + i_{q2}\right] + L_m\left[-i_{q1} - i_{q2} + i_{qr}\right] \tag{14}$$

$$\lambda_{d2} = -L_{12} i_{d2} - L_{lm}\left[i_{d1} + i_{d2}\right] + L_m\left[-i_{d1} - i_{d2} + i_{dr}\right] \tag{15}$$

$$\lambda_{qr} = L_{lr} i_{qr} + L_m\left[-i_{q1} - i_{q2} + i_{qr}\right] \tag{16}$$

$$\lambda_{dr} = L_{lr} i_{dr} + L_m\left[-i_{d1} - i_{d2} + i_{dr}\right] \tag{17}$$

Where $L_{lm}$ common mutual leakage inductance between the two is sets of stator winding and the magnetizing inductance and $L_m$ depends on the degree of saturation. It is non linear function of the magnetizing current $i_m$, which can be obtained from the magnetization curve of the machine. These variables represent in equations are given below,

$$L_{lm} = L_{lax}\cos\alpha + L_{lay}\cos\left(\alpha + 2\Pi/3\right) + L_{laz}\cos\left(\alpha - 2\Pi/3\right) \tag{18}$$

$$L_m = \left(\lambda_m / i_m\right) \tag{19}$$

$$L_r =_{Llr} + L_m \tag{20}$$

The common mutual leakage inductance $L_{lm}$ is defined as the fact two sets of stator windings occupy the same slots and mutually coupled by a component of leakage flux. This mutual leakage inductance $L_{lm}$ has been produced by an important effect on the harmonic coupling between the two-stator winding sets and also depends on the winding pitch and the displacement angle between two-stator winding sets.

In the above all equation suggests the equivalent circuit is shown in figure 5 and the corresponding prime quantities are referred to stator. The transient behavior is concerned for founding out for neglecting

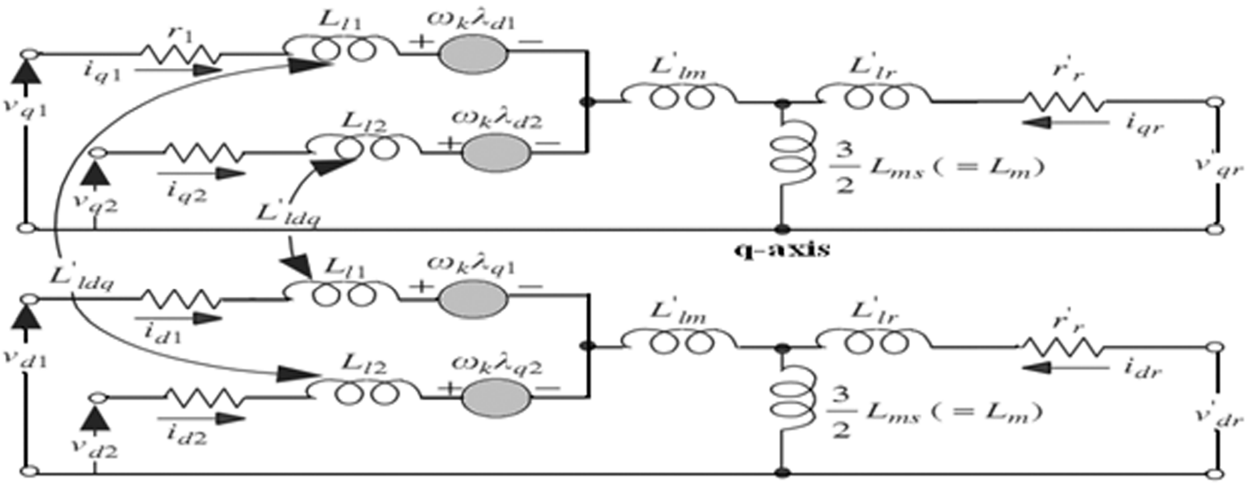

**Figure 5: D-q axis Equivalent Circuit of six phase induction machine in arbitrary reference frame**

the stator mutual leakage reactance. The detailed simulation of six phase induction machine based on the arbitrary reference frame may be demonstrated by first solving the flux linkage equation for the current equations are obtained below,

$$i_{q1} = \frac{1}{L_l}\left\{\left(L_{lm} + L_{12}\right)\lambda_{q1} - L_{lm}\lambda_{q2} - L_{12}\lambda_{mq}\right\} \tag{21}$$

$$i_{d1} = \frac{1}{L_l}\left\{\left(L_{lm} + L_{12}\right)\lambda_{d1} - L_{lm}\lambda_{d2} - L_{12}\lambda_{md}\right\} \tag{22}$$

$$i_{q2} = \frac{1}{L_l}\left\{\left(L_{lm} + L_{11}\right)\lambda_{q2} - L_{lm}\lambda_{q1} - L_{11}\lambda_{mq}\right\} \tag{23}$$

$$i_{d2} = \frac{1}{L_l}\left\{\left(L_{lm} + L_{11}\right)\lambda_{d2} - L_{lm}\lambda_{d1} - L_{11}\lambda_{md}\right\} \tag{24}$$

$$i_{qr} = \frac{\lambda_{qr}}{L_{lr}} - \frac{\lambda_{mq}}{L_{lr}} \tag{25}$$

$$i_{dr} = \frac{\lambda_{dr}}{L_{lr}} - \frac{\lambda_{md}}{L_{lr}} \tag{26}$$

The detailed simulation of a multi-phase machine is based on the integral form of the machine's voltage and torque equations with flux linkage and speed as state variables, winding currents as output variables, applied voltage and load torque as input variables. To solving for the currents and back substituting of currents into the voltage equations and rewriting as differential equations are given by,

$$p\lambda_{q1} = \left\{v_{q1} - \frac{r_1}{L_l}\left(\left[L_{lm} + L_{12}\right]\lambda_{q1} - L_{lm}\lambda_{q2} - L_{12}\lambda_{mq}\right) + \omega_k\lambda_{d1}\right\} \tag{27}$$

$$p\lambda_{d1} = \left\{v_{d1} - \frac{r_1}{L_l}\left(\left[L_{lm} + L_{12}\right]\lambda_{d1} - L_{lm}\lambda_{d2} - L_{12}\lambda_{md}\right) - \omega_k\lambda_{q1}\right\} \tag{28}$$

$$p\lambda_{q2} = \left\{v_{q2} - \frac{r_2}{L_l}\left(\left[L_{lm} + L_{11}\right]\lambda_{q2} - L_{lm}\lambda_{q1} - L_{11}\lambda_{mq}\right) + \omega_k\lambda_{d2}\right\} \tag{29}$$

$$p\lambda_{d2} = \left\{v_{d2} - \frac{r_2}{L_l}\left(\left[L_{lm} + L_{11}\right]\lambda_{d2} - L_{lm}\lambda_{d1} - L_{11}\lambda_{md}\right) - \omega_k\lambda_{q2}\right\} \tag{30}$$

$$p\lambda_{qr} = \left\{\left(-\left[\omega_k - \omega_r\right]\lambda_{dr} - \frac{r_r}{L_{lr}}\left[\lambda_{qr} - \lambda_{mq}\right]\right)\right\} \tag{31}$$

$$p\lambda_{dr} = \left\{\left(\left[\omega_k - \omega_r\right]\lambda_{qr} - \frac{r_r}{L_{lr}}\left[\lambda_{dr} - \lambda_{md}\right]\right)\right\} \tag{32}$$

Where,

$$\lambda_{mq} = A\left[\frac{\left(L_{12}\lambda_{q1} + L_{11}\lambda_{q2}\right)}{(L)} + \left(\frac{\lambda_{qr}}{L_{lr}}\right)\right] \tag{33}$$

$$\lambda_{md} = A\left[\frac{\left(L_{12}\lambda_{d1} + L_{11}\lambda_{d2}\right)}{(L)} + \left(\frac{\lambda_{dr}}{L_{lr}}\right)\right] \tag{34}$$

$$A = 1/\left[\left(\frac{1}{L_m}\right) + \left(\frac{1}{L_{lr}}\right) + \left(\frac{L_{11} + L_{12}}{L}\right)\right] \tag{35}$$

$$L = \left[L_{11}L_{12} + L_{lm}\left(L_{11} + L_{12}\right)\right] \tag{36}$$

The rotor dynamics and torque equations can be given as,

$$\left(\omega_r / \omega_b\right) = (1/p)\left[\left(1 - \omega_b\right)(P/2)(1/J)\left(T_{em} - T_{sh}\right)\right] \tag{37}$$

$$T_{em} = (3/2)(P/2)\left(L_m / L_r\right)\left[\left(i_{q1} + i_{q2}\right)\lambda_{dr} - \left(i_{d1} - i_{d2}\right)\lambda_{qr}\right] \tag{38}$$

Where, P is denoting the number of poles, J is mention the moment of inertia, $\omega_b$ is represent the base speed (rad/s) and $T_{sh}$ is denote the shaft torque. The value of magnetic inductance depends on the degree of magnetic saturation. It is a nonlinear function of magnetic current. Also, it can be expressed in the following equation and the magnetizing inductance. It is calculated from the magnetizing characteristics and can be obtained by synchronous speed test of the machine equations. The corresponding equations are given below,

$$i_m = \sqrt{\left(-i_{q1} - i_{q2} + i_{qr}\right)^2 + \left(-i_{d1} - i_{d2} + i_{dr}\right)^2} \tag{39}$$

$$L_m = a_0 + a_1 i_m + a_2 i_m^2 + a_3 i_m^3 \tag{40}$$

In general the first utilizes of current as state space variables, while the other relies on d–q axis flux components as state space variables. Where, a0, a1, a2 and a3 are constants and are given in table 1. The modeling of excitation capacitor and various load condition can be discussed in below section.

### 4.1. Modeling of shunt excitation capacitor

The voltage and current equations of excitation capacitor can be transformed from three-phase quantities into d–q axis by using Krause transformation [3] and related equations are given by,

$$pv_{q1} = \left(i_{q1c} / C_{sh1}\right) - \omega_b v_{d1} \tag{41}$$

$$pv_{d1} = \left(i_{d1c} / C_{sh1}\right) + \omega_b v_{q1} \tag{42}$$

$$pv_{q2} = \left(i_{q2c} / C_{sh2}\right) - \omega_b v_{d2} \tag{43}$$

$$pv_{d2} = \left(i_{d2c} / C_{sh2}\right) + \omega_b v_{q2} \tag{44}$$

where $i_{q1c}$, $i_{d1c}$, $i_{q2c}$ and $i_{q1c}$ are denoting the q- and d-axis components of currents flowing into the exciter capacitor and $C_{sh1}, C_{sh2}$ are represented by across the three-phase winding set I and II respectively.

## 4.2. Modeling of series excitation capacitor

The modeling of current through series capacitor $C_{se1}, C_{se2}$ has connected in winding set I and II respectively as same as the load current. The load current along with series capacitance can be used to determine the voltage across series capacitor and then transformed into d–q axis is given by,

$$pv_{q1se} = i_{q1L/C_{se1}} \tag{45}$$

$$pv_{d1se} = i_{d1L/C_{se1}} \tag{46}$$

$$pv_{q2se} = i_{q2L/C_{se2}} \tag{47}$$

$$pv_{d2se} = i_{d2L/C_{se2}} \tag{48}$$

Where the load terminal voltage equations are expressed as given below,

$$v_{Lq1} = v_{q1} - v_{q1se} \tag{49}$$

$$v_{Ld1} = v_{d1} - v_{d1se} \tag{50}$$

$$v_{Lq2} = v_{q2} - v_{q2se} \tag{51}$$

$$v_{Ld2} = v_{d2} - v_{d2se} \tag{52}$$

## 4.3. Modeling of Various Static Load Conditions

### *4.3.1. Purely Resistive Load (R) Condition*

If a purely resistive load is connected across the terminal of the generator, the load current (without series capacitor) can be given by,

$$i_{d1L} = v_{d1} / R_1 \;\;\&\;\; i_{q1L} = v_{q1} / R_1 \tag{53}$$

$$i_{d2L} = v_{d2} / R_2 \;\;\&\;\; i_{q2L} = v_{q2} / R_2 \tag{54}$$

The Applying Kirchhoff's current law at capacitor terminals side, to current flowing through the shunt capacitor will be given as,

$$i_{q1c} = i_{q1} - i_{q1L} \;\;\&\;\; i_{d1c} = i_{d1} - i_{d1L} \tag{55}$$

$$i_{q2c} = i_{q2} - i_{q2L} \;\;\&\;\; i_{d2c} = i_{d2} - i_{d2L} \tag{56}$$

So that the modified voltage equations with purely resistive load are given below,

$$pv_{q1} = \left(i_{q1} / C_{sh1}\right) - \left(v_{q1} / \left(R_1 C_{sh1}\right)\right) - \omega_b v_{d1} \tag{57}$$

$$pv_{d1} = \left(i_{d1} / C_{sh1}\right) - \left(v_{d1} / \left(R_1 C_{sh1}\right)\right) + \omega_b v_{q1} \tag{58}$$

$$pv_{q2} = \left(i_{q2} / C_{sh2}\right) - \left(v_{q2} / \left(R_2 C_{sh2}\right)\right) - \omega_b v_{d2} \tag{59}$$

$$pv_{d2} = \left(i_{d2} / C_{sh2}\right) - \left(v_{d2} / \left(R_2 C_{sh2}\right)\right) + \omega_b v_{q2} \tag{60}$$

where $R_1$ and $R_2$ are the load resistances connected across the winding set I and II respectively.

### *4.3.2.* Lagging Power Factor Load (RL) Condition

In general, assume the load is consider as $R_1 L_1$ and $R_2 L_2$ (per phase value) series circuit connected across winding set I and II respectively. The voltage equations will be given as,

$$pv_{q1} = \left(i_{q1} / C_{sh1}\right) - \left(i_{q1L} / C_{sh1}\right) \tag{61}$$

$$pv_{d1} = \left(i_{d1} / C_{sh1}\right) - \left(i_{d1L} / C_{sh1}\right) \tag{62}$$

$$pv_{q2} = \left(i_{q2} / C_{sh2}\right) - \left(i_{q2L} / C_{sh2}\right) \tag{63}$$

$$pv_{d2} = \left(i_{d2} / C_{sh2}\right) - \left(i_{d2L} / C_{sh2}\right) \tag{64}$$

Where the q and d axis of load current can be expressed as given by,

$$pi_{q1L} = \left(v_{q1} / L_1\right) - \left(R_1 / L_1\right)\left(i_{q1L}\right) \tag{65}$$

$$pi_{d1L} = \left(v_{d1} / L_1\right) - \left(R_1 / L_1\right)\left(i_{d1L}\right) \tag{66}$$

$$pi_{q2L} = \left(v_{q2} / L_2\right) - \left(R_2 / L_2\right)\left(i_{q2L}\right) \tag{67}$$

$$pi_{d2L} = \left(v_{d2} / L_2\right) - \left(R_2 / L_2\right)\left(i_{d2L}\right) \tag{68}$$

### *4.3.3.* Model of RLC Load Condition

The dynamic model of three phase RLC load condition in the arbitrary reference frame is given as,

$$i_{ld1} = \left(\int \left(\frac{1}{L_1}\right) v_{ld1} - \left(\frac{R_1}{L_1}\right) i_{ld1} - \left(\frac{1}{L_1 c_1}\right) \int i_{ld1}\right) \tag{69}$$

$$i_{lq1} = \left(\int \left(\frac{1}{L_1}\right) v_{lq1} - \left(\frac{R_1}{L_1}\right) i_{lq1} - \left(\frac{1}{L_1 c_1}\right) \int i_{lq1}\right) \tag{70}$$

$$i_{ld2} = \left(\int \left(\frac{1}{L_2}\right) v_{ld2} - \left(\frac{R_2}{L_2}\right) i_{ld2} - \left(\frac{1}{L_2 c_2}\right) \int i_{ld2}\right) \tag{71}$$

$$i_{lq2} = \left(\int \left(\frac{1}{L_2}\right) v_{lq2} - \left(\frac{R_2}{L_2}\right) i_{lq2} - \left(\frac{1}{L_2 c_2}\right) \int i_{lq2}\right) \tag{72}$$

Where $i_{ld1}, i_{lq1}$ denotes load currents in the d-q axis for winding set abc, $i_{ld2}, i_{lq2}$ denotes load currents in the d-q axis for winding set xyz, $R_1, L_1, C_1$ are represent the load resistance, load inductance and capacitance for winding set abc and $R_2, L_2, C_2$ are represent the load resistance, load inductance and capacitance for winding set xyz.

## 5. DYNAMIC ANALYSIS OF SIX PHASES SEIG

The analytical studies of six phases self excited induction generator have been carried out by using MATLAB/SIMULINK. The complete simulation model of the SPSEIG driven by fixed pitch wind turbine is shown in

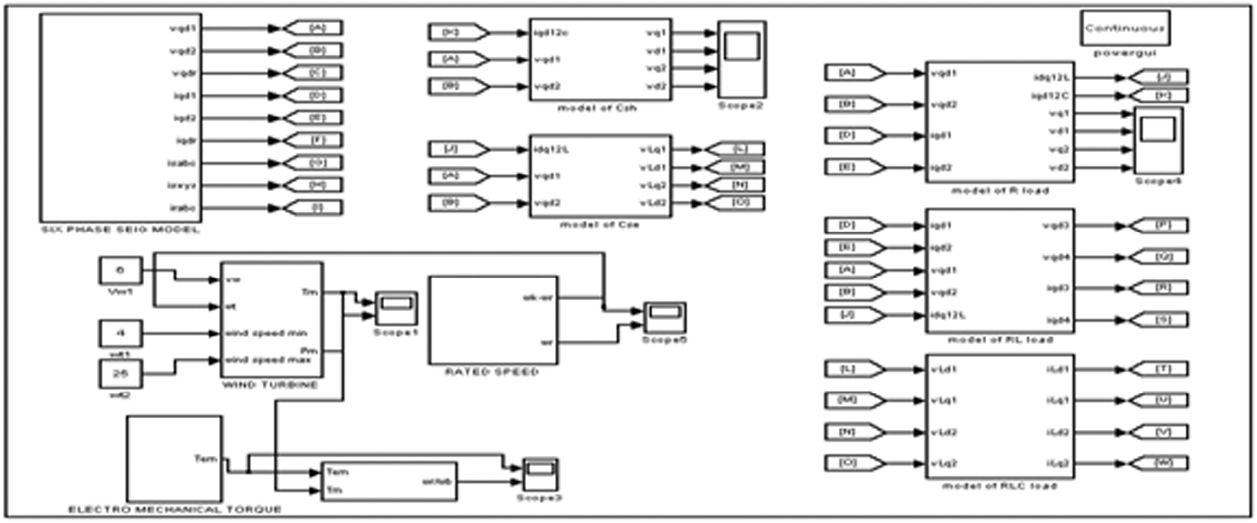

Figure 6: Simulink Model of Wind Driven SPSEIG with Various Load Condition

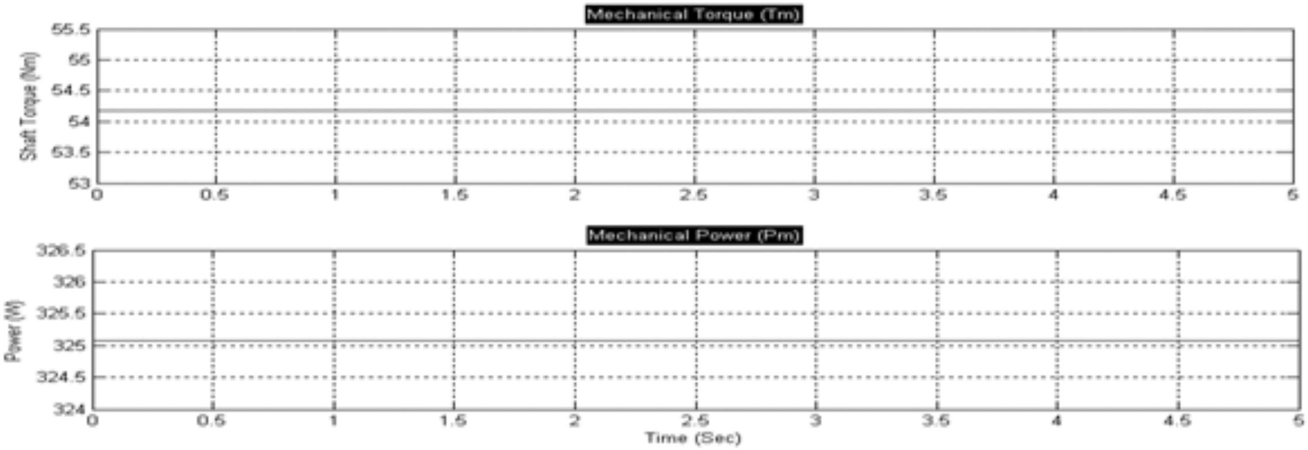

Figure 7: Mechanical torque and power waveform of wind turbine

figure. The mathematical modeling of overall blocks consists as wind turbine, SPSEIG, Electro Mechanical torque, Rated speed and various static load conditions. The interaction between of two windings is representing the destiny and variation of the load. It acts on one winding changes operating conditions to the other winding situation. It is still maintain for a wide range of rural resistive loads. The overall simulink model of wind driven SPSEIG with different load conditions is shown below in figure 6.

The fixed pitch wind turbine has been analyzed and generation of mechanical torque and power is shown in figure. Normally, an induction motor contain the rotor rotates at a slower speed than the stator field. So becomes the stator voltage and frequency is higher, while compare to that rotor voltage and frequency. The mathematical modeling of SPSEIG simulation can be obtained waveform listed as six phase input voltage, torque, rated speed and power is shown in figures 7, 8, 9, 10.

The parameters of the test machine are given in Appendix I and this study explained the effect of cross saturation has been neglected. The dynamic performances have been presented under following operating conditions such as,

i. Voltage and Current Build-up of six phases SEIG at no load.
ii. Dynamic responses under resistive (R) load condition with and without series compensation.
iii. Dynamic responses under RL load condition with and without series compensation.
iv. Dynamic responses under RLC load condition with and without series compensation.

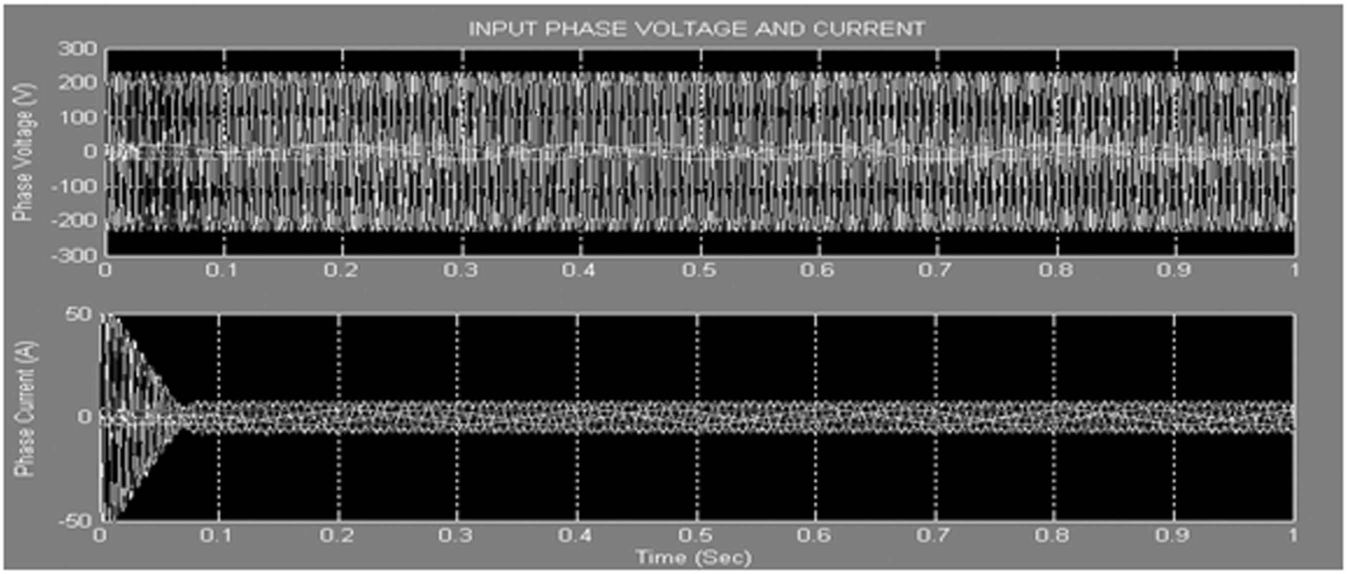

**Figure 8: Six phase input voltage and current waveform**

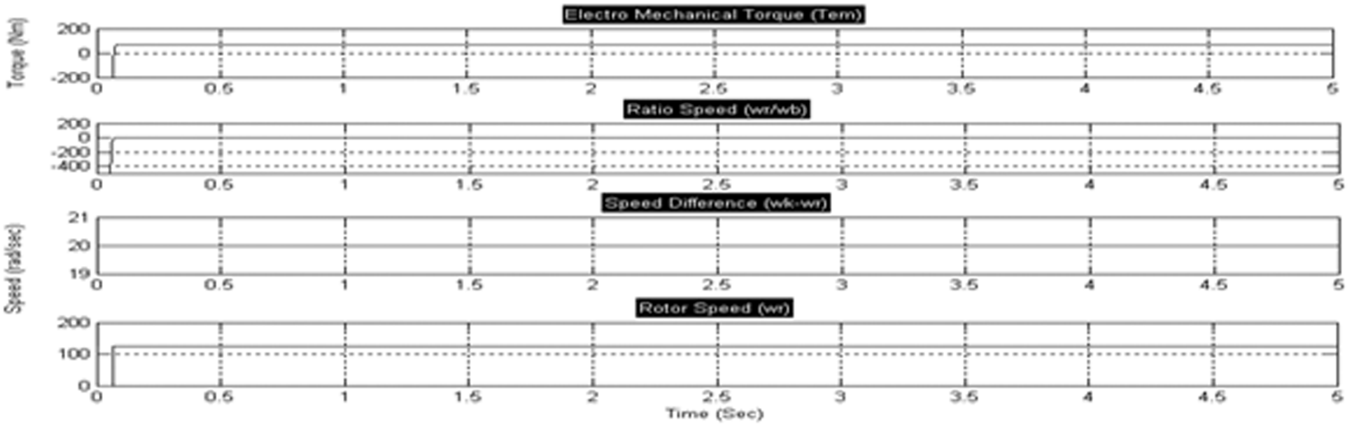

**Figure 9: SP-SEIG performance waveform**

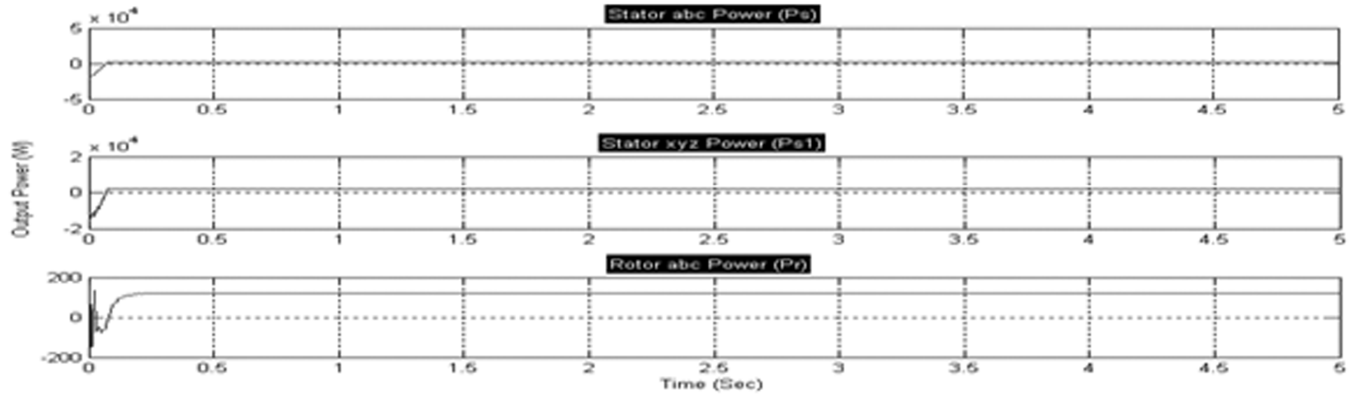

**Figure 10: Stator and Rotor Power Waveform of SP-SEIG**

## 5.1. Voltage and Current Build up at no load

In this paper, for taken per phase value of shunt excitation capacitor selected as 38.5μ*F*. The analytical response waveform of voltage and current during at no load condition for the two three phase winding set is shown in figures 11. The steady state no-load voltage is generated by 230V at rated speed of 1000rpm. It can be observed by the SEIG terminal voltage and current build-up from the initial value of few volts and

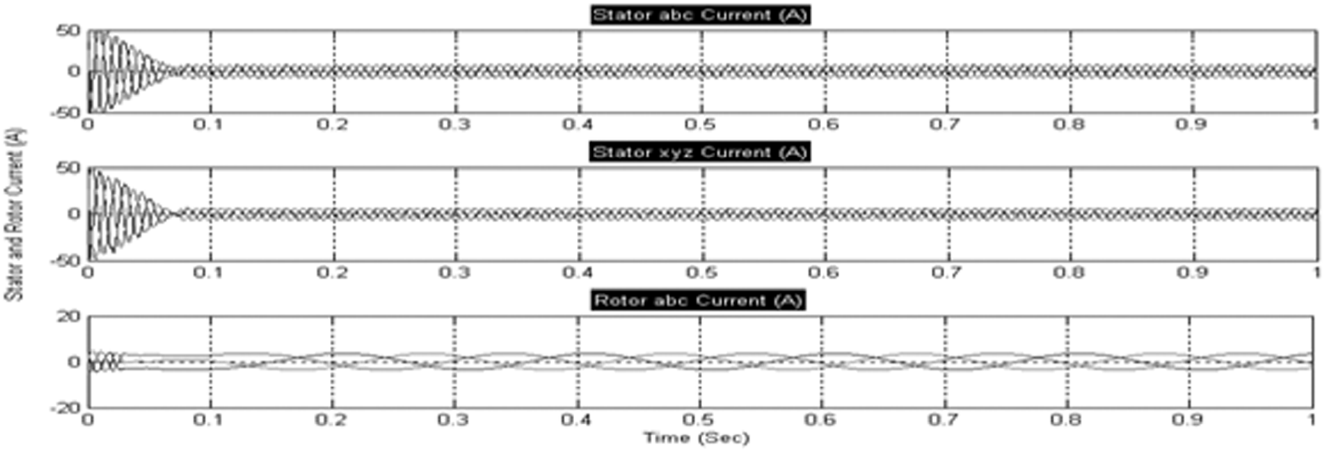

Figure 11: (a) Current build up of SPSEIG at no load

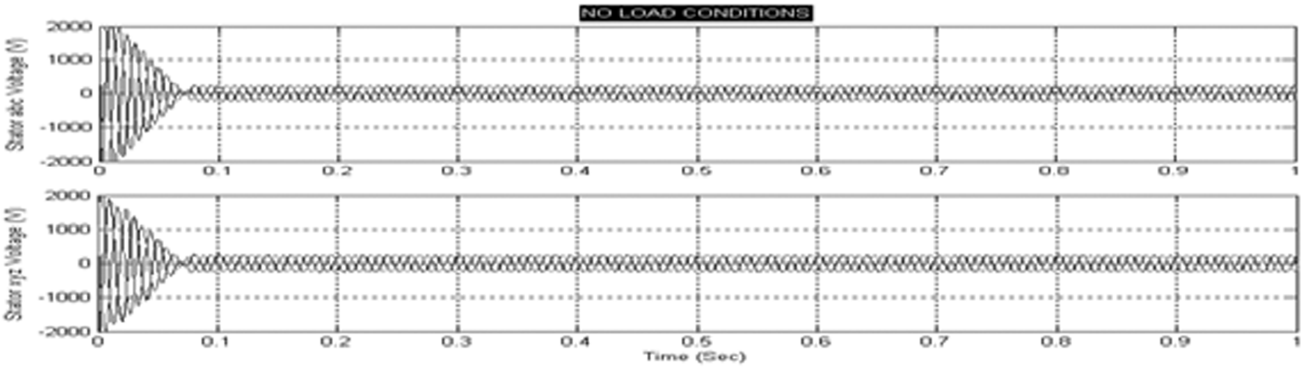

Figure 11: (b) Voltage Build up of SPSEIG at no load

few amperes to the steady state values. Furthermore, the magnitude of the voltage is much higher in case of a higher capacitor. In order to effect of the excitation current increases with the increase in excitation capacitance. The rate of no-load voltage and current build- up is depends upon the value of shunt excitation capacitance and also the level of residual magnetism in the rotor circuit of the SEIG.

### 5.2. Transient response under R load with and without Series compensation

The simulated dynamic response of six-phase SEIG terminal voltage and load current at switching in a resistive load of 600Ω. The sudden change of the resistive load and the terminal voltage are reduced to 100V. It gives the decrease in terminal voltage and also causes a decrease in excitation capacitor current. It can be affects the voltage regulation of the generator. The poor voltage regulation of the SEIG is taken as due to lack of reactive power. So that it can be compensated through by using the series capacitor connected in each line. The voltage waveform under R load conditions with and without series compensation is shown in figures 12.

To selection of the value of shunt and series capacitors may be avoid the excessive voltage at SEIG terminals. The application of series capacitor should be used in an over-voltage across the generator terminals. Moreover, the selection of series capacitance should be justified not only for the basis of full load voltage regulation but also obtained from the view point of load voltage profile and maximum utilization of the machine as the generator. The dynamic response of six phases SEIG feeding a resistive load of 600Ω and likewise the series capacitors $10\mu F$ are connected in each line between load and SEIG. Almost, here retains the no load voltage because of self regulating reactive power the load. In order to carry out the drop in SEIG terminal voltage, becomes less susceptible to sudden loading conditions as result of series compensation.

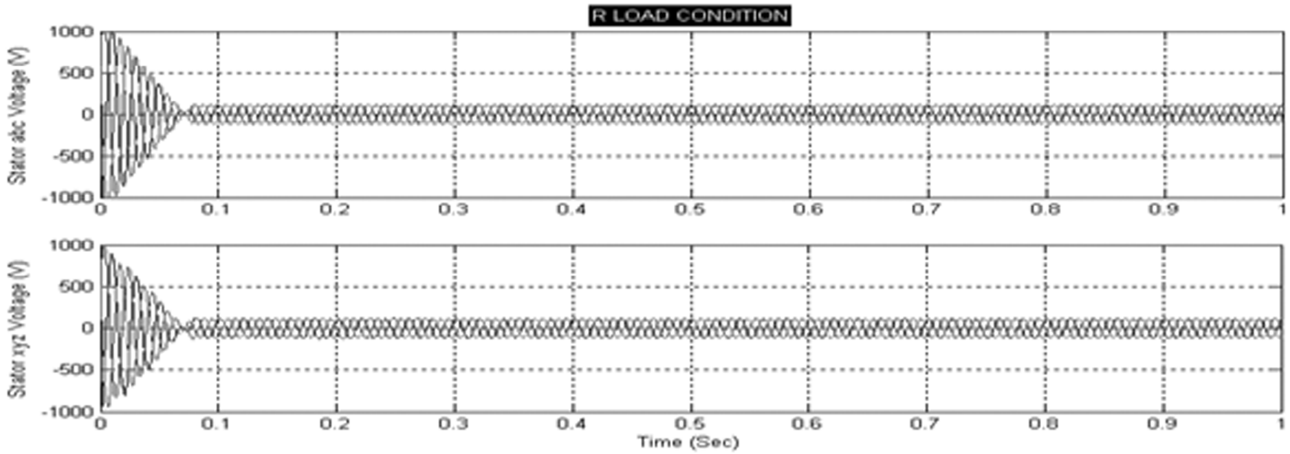

**Figure 12: (a) Voltage waveform at R load without series compensation**

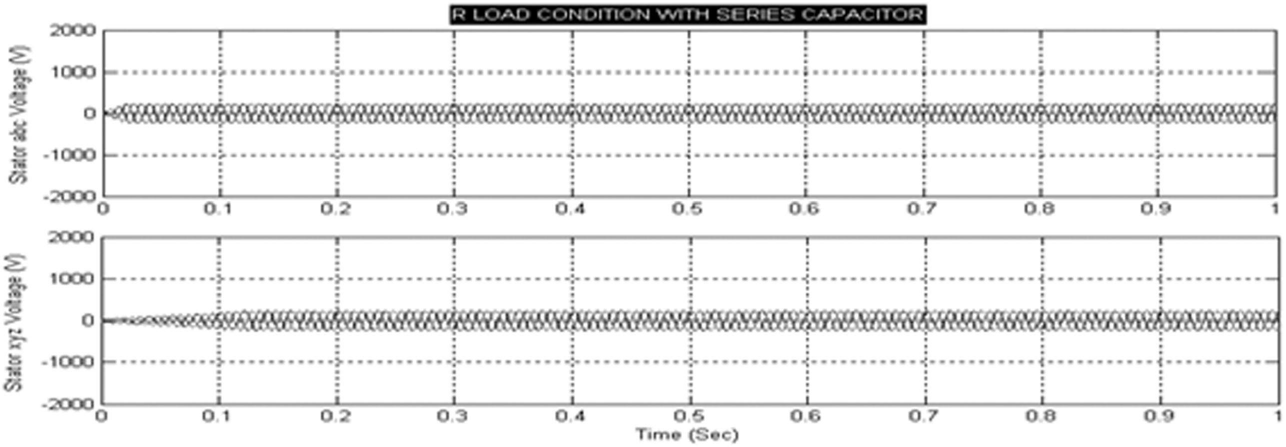

**Figure 12: (b) Voltage waveform at R load with series compensation**

## 5.3. Transient Response under RL load with and without series compensation

The lagging power factor load test is performed with a balanced three-phase RL load comprising 200Ω resistance in series with 500mH inductor. The generator voltage has been dropped to 80V. The dynamic response of six phases SEIG at terminal voltage under reactive load without and with series capacitor is shown in figures 13.

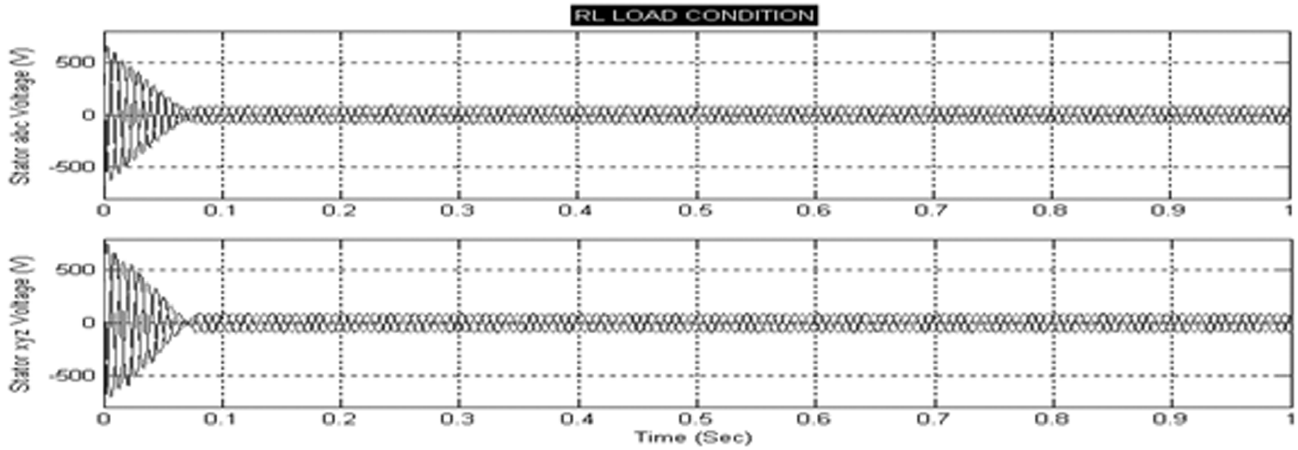

**Figure 13: (a) Voltage waveform at RL load without series compensation**

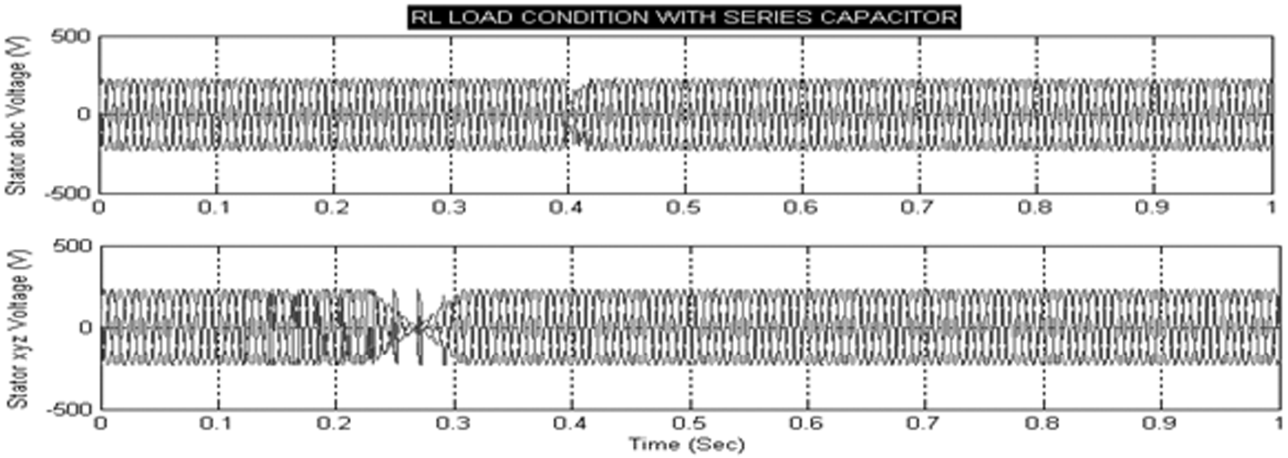

**Figure 13: (b) Voltage waveform at RL load with series compensation**

In generally, SEIG with constant speed and rotating magnetic field lags behind the rotor speed. In order to increase in load of the SEIG consider, while magnitude of the negative slip increases. In this study as the rotor speed is denoted as the input and increase with slip due to the decrease in the speed of the rotating magnetic field. The SEIG retains of no load voltage due to the reactive power provided by the selection of series capacitors range as $10\mu F$. Thus, the generated voltage and frequency are proportional to the speed of rotating magnetic field and also decrease in the speed of rotating magnetic field.

### 5.4. Transient Response under RLC load with and without series compensation

The transient performance of the SPSEIG system based balanced load condition such as RLC $(150\Omega, 0.08H, 12\mu F)$. It can be obtained that the terminal voltage and current attain their steady-state operation. Becomes, the generator voltage has been dropped to 40V. The dynamic response of six phases SEIG under RLC load with without series compensation waveform is shown in figures 14.

In order to connection of load can be affected to the dynamic response of SPSEIG output voltage. Under RLC load effect on the SPSEIG output voltage can be compensated using a series capacitor. The proper selection of series capacitor should be used as $10\mu F$. This low value of the series capacitor can be assign relative to the load impedance and power factor. With a proper choice of series and shunt capacitors must use as the quality of output voltage and current waveforms can also be controlled. The series capacitor should be used as the load for an appropriate capacitance value. So becomes that sufficient excitation of the SPSEIG can be maintained when the load is connected. Similarly, the higher-value capacitor will be over exciting the SPSEIG and the output voltage could be reach high values.

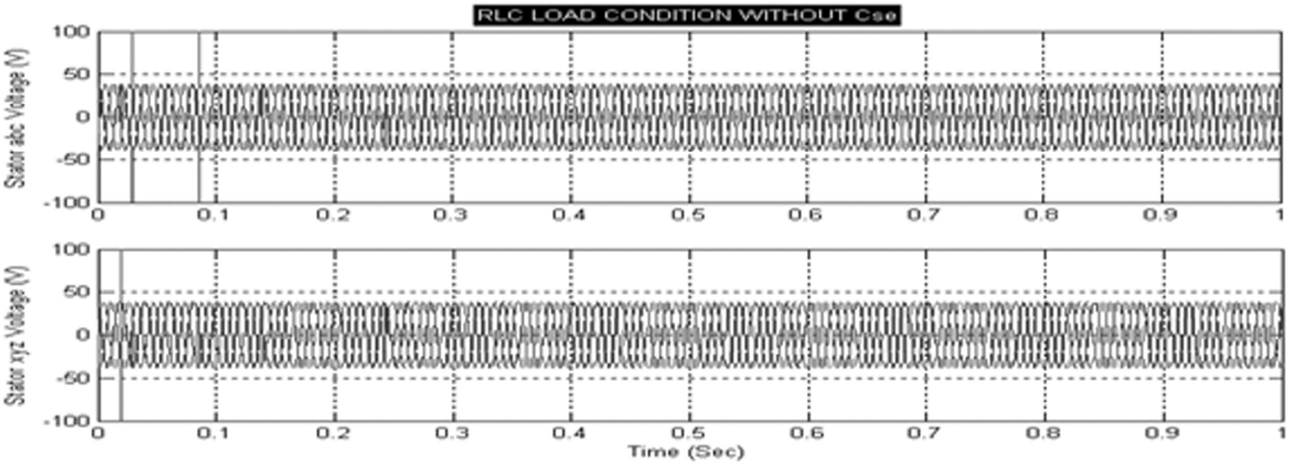

**Figure 14: (a) Voltage waveform at RLC load without series compensation**

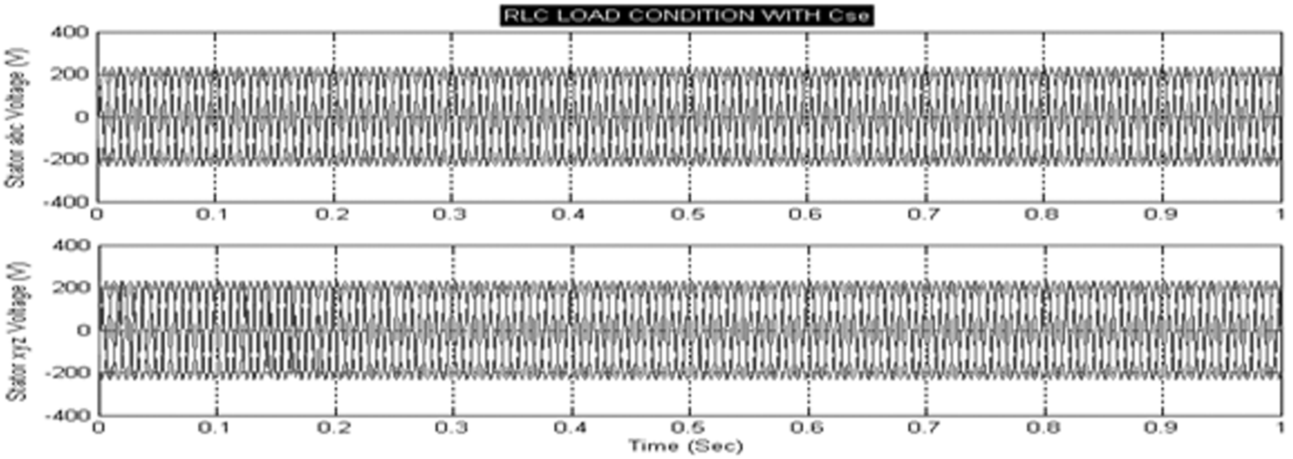

Figure 14: (b) Voltage waveform at RLC load with series compensation

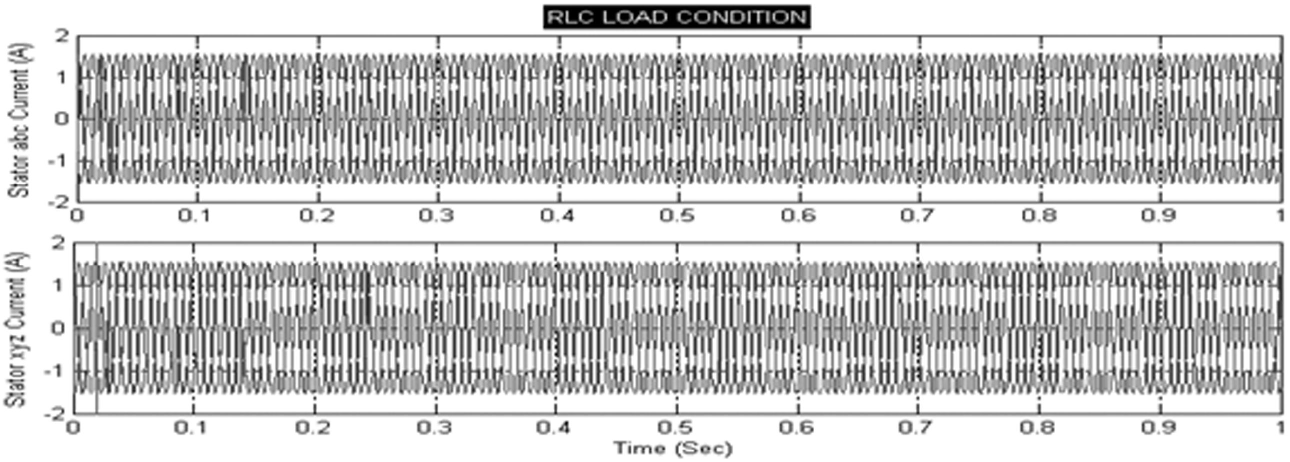

Figure 14: (c) Current waveform at RLC load with series compensation

**Table 1**
**Induction Machine Parameter Specification**

| Parameters | Values |
|---|---|
| Stator Resistance ($r_1$, $r_2$) | 4.12Ω |
| Stator Leakage Inductance ($L_{11}$, $L_{12}$) | 21.6mH |
| Rotor Resistance ($r_r$) | 8.79Ω |
| Rotor Leakage Inductance ($L_{1r}$) | 43.3mH |
| Mutual Leakage Inductance ($L_{lm}$) | 234.6mH |
| Magnetization constants ($a_1$, $a_2$, $a_3$, $a_4$) | 0.1031 |
| | 0.019 |
| | -0.004 |
| | 0.0002 |

## 6. CONCLUSION

This paper has been presented, the simple d–q model of a saturated multi-phase (six-phase) self-excited induction generator (SP-SEIG) driven by a fixed pitch wind turbine under no-load connection with different excitation capacitors and under a various balanced load condition. In the analytical study model of dynamic cross saturation and the effects of common mutual leakage inductance between the two three-phase winding sets have been analyzed. The performance of generator under different capacitor excitation values is verified.

This corresponding result can be indicate the high excitation capacitance values lead to rapid voltage build up and higher values of the output voltage. Moreover, an appropriate combination of series and shunt capacitors are necessary to achieve the desired level of voltage regulation, to keeping the machine voltage and current within specified limits. This proposed model is equally applicable to the machine with any arbitrary phase displacement between the two winding sets. Hence, in order verified the voltage/current regulation, power handling capacity and efficiency of SP-SEIG.

## REFERENCES

[1] Farrag, Mohamed EA, and Ghanim A. Putrus. "Analysis of the Dynamic Performance of Self-Excited Induction Generators Employed in Renewable Energy Generation." *Energies*, vol. 7, no. 1, pp. 278-294, 2014.

[2] Ahuja, R.K.; Murthy, S.S.; Chaudhary, J.K., "Steady state analysis of three phase self excited induction generator using MATLAB GUI to feed single phase loads with three capacitor configuration," *IEEE 5th India International Conference on Power Electronics (IICPE),* vol.1, no.6, pp. 6-8, Dec. 2012.

[3] Singh, G. K. "Modeling and experimental analysis of a self-excited six-phase induction generator for stand-alone renewable energy generation." *Renewable energy, vol.* 33, no. 7, pp. 1605-1621, 2008.

[4] Palle, B.; Simoes, M.G.; Farret, F.A., "Dynamic simulation and analysis of parallel self-excited induction generators for islanded wind farm systems," *IEEE Transactions on Industry Applications,* vol.41, no.4, pp.1099-1106, July-Aug. 2005.

[5] Li Wang; Jian-Yi Su, "Dynamic performances of an isolated self-excited induction generator under various loading conditions," *IEEE Transactions on Energy Conversion,* vol.14, no.1, pp.93-100, Mar 1999.

[6] Renukadevi, G., and K. Rajambal. "Generalized dq Model of n-Phase Induction Motor Drive." *International Journal of Electrical, Electronic Science and Engineering, vol.* 6, no. 9, 2012.

[7] Nounou, K.; Marouani, K.; Benbouzid, M.; Tabbache, B., "Six-phase induction machine operating as a standalone self-excited induction generator," *2014 International Conference on Green Energy,* vol.158, no.163, pp. 25-27, March 2014.

[8] Moulahoum, Samir, and Nadir Kabache. "Behaviour Analysis of Self Excited Induction Generator Feeding Linear and No Linear Loads." *Journal of Electrical Engineering & Technology*, vol. 8, no. 6, pp. 1371-1379, 2013.

[9] Nazir, Refdinal. "Analysis of Harmonic Currents Propagation on the Self-Excited Induction Generator with Nonlinear Loads." *Journal of Electrical Engineering & Technology, vol.* 9, no. 6, pp. 1935-1943, 2014.

[10] Singh, Bhim, S. S. Murthy, and Sushma Gupta. "A Solid State Controller for Self-Excited Induction Generator for Voltage Regulation, Harmonic Compensation and Load Balancing." *Journal of Power Electronics, vol.* 5, no. 2, pp. 109-119, 2005.

[11] Kim, Chan-Ki, Young-Do Choy, and Seong-Joo Lim. "Transient simulation of a self-excited induction generator during grid faults." *Journal of Power Electronics, vol.* 7, no. 2, pp. 89-96, 2007.

[12] Kamil, Haval Sardar, and S. U. Kulkarni. "Overview of Wind Turbine Driven Self-Excited Induction Generator." *International Journal of Innovative Technology and Exploring Engineering (IJITEE), Vol.2, no-4, pp. 181-185, March 2013.*

[13] Singh, G.K.; Kumar, A.S.; Saini, R.P., "Selection of capacitor for the self-excited six-phase induction generator," *International Conference on Power Systems, ICPS '09,* vol.1, no.6, pp. 27-29, Dec. 2009.

[14] Singh, P.K.; Chauhan, Y.K., "Performance analysis of multi-pulse electronic load controllers for self-excited induction generator," *International Conference on Energy Efficient Technologies for Sustainability (ICEETS),* vol.1299, no.1307, pp. 10-12, April 2013.

[15] Murthy, S.S.; Bhuvaneswari, G.; Gao, S.; Ahuja, R.K., "Self excited induction generator for renewable energy applications to supply single-phase loads in remote locations," *IEEE International Conference on Sustainable Energy Technologies (ICSET),* vol.1, no.8, pp. 6-9, Dec. 2010.